Chemical Engineering Journal 160 (2010) 383–390

Contents lists available at ScienceDirect

Chemical Engineering Journal

journal homepage: www.elsevier.com/locate/cej

PEDOT/Nafion composite thin films supported on Pt electrodes: Facile fabrication and electrochemical activities

Peng Wang[a,*], William L. Olbricht[a,b]

[a] *School of Chemical and Biomolecular Engineering, Cornell University, Ithaca, NY 14853, USA*
[b] *Department of Biomedical Engineering, Cornell University, Ithaca, NY 14853, USA*

ARTICLE INFO

Article history:
Received 13 December 2009
Received in revised form 5 March 2010
Accepted 19 March 2010

Keywords:
PEDOT
Nafion
Electrochemical polymerization
EFM
Overoxidation
Hole mobility

ABSTRACT

Poly-3,4-ethylenedioxythiophene(PEDOT)/Nafion composite thin films were prepared by a facile electrochemical polymerization approach. These films were characterized by wavelength dispersive spectroscopy (WDS), scanning electron microscopy (SEM), atomic/electric force microscopy (AFM/EFM), cyclic voltammetry (CV), potential step chronoamperometry (PSC), and electrochemical impedance spectroscopy (EIS). The as-prepared film was dense and smooth and had nearly uniform PEDOT and Nafion distribution on the nanometer scale with slight localized phase segregation. Electrochemical experiments revealed a PEDOT/Nafion stable potential window and a PEDOT/Nafion overoxidation potential window. Hole mobility in the film was quantified by PSC technique and charge transport theory, and was verified independently by EIS technique.

1. Introduction

Electronically conducting polymers have in recent years become more and more useful in electrical and electronic devices. PEDOT, in particular, has many unusual and outstanding properties [1,2]. For example, the dioxyethylene bridging group across the 3- and 4-positions of the heterocycle can block α–β' coupling and structural disorder and thereby renders PEDOT excellent electrochemical stability [3]. The dioxyethylene bridge also gives the PEDOT a lower band gap compared to thiophene, resulting in lower monomer and polymer oxidation potentials [4]. Doped PEDOT displays electronic conductivities ranging from 1 to 100 S/cm, depending on the dopants [4,5]. In addition, improved thermal stability of PEDOT relative to other polyheterocycles has been demonstrated [6–8].

On the other hand, ionomers, i.e. ion containing polymers, have drawn attentions both from academia and industry since 1940s. Nafion is the most well known one. Nafion consists of a polytetrafluoroethylene backbone and a perfluorovinyl ether pendant side chain terminated by a sulfonate ionic group. One of the well-adopted structural models for Nafion describes its microscopic structure as clusters interconnected by narrow channels which determine the transport properties of ions and water [9]. Nafion is highly conductive to cations such as protons and belongs to the wide class of solid superacid catalysts.

The combination of PEDOT and Nafion might lead to interesting electronic and ionic properties. PEDOT/Nafion composites have been scarcely studied. Higgins et al. [10] prepared and characterized PEDOT films coated onto fluorocarbon membranes containing sulfonate groups, such as Nafion and poly(styrene-4-sulfonate)-grafted poly(vinylidene fluoride) membranes. Li et al. [11] modified Nafion membranes with a thin film of PEDOT by a diffusion-controlled polymerization process using a two-compartment cell with the monomer EDOT on one side of the membrane and the oxidizing agent $FeCl_3$ on the other side, and further measured the methanol permeability and ion conductivity of the composite membranes as a function of temperature and polymerization time. In both work, PEDOT was formed by chemical oxidation of 3,4-ethylenedioxythiophene (EDOT) on a pre-fabricated Nafion or Nafion containing membrane. These experiments were carried out for long time durations and with multiple chemicals and the electrochemical properties of the fabricated membranes were difficult to be studied. Besides, in these composites PEDOT and Nafion essentially existed in two bulk phases separated by a phase boundary. Composites with the two species mixed on the nanometer or even on the molecular level have not been achieved yet. This was partly due to the difficulty and complexity in dissolving Nafion in a solvent since Nafion, as a fluoropolymer, has a high resistance to solvent. In this paper, we report a facile approach to the fabrication and electrochemical characterization of PEDOT/Nafion composite thin films. In these films, PEDOT and Nafion can be considered to a large

---

* Corresponding author at: 120 Olin Hall, Cornell University, Ithaca, NY 14853, USA. Tel.: +1 607 342 8522; fax: +1 607 255 9166.
E-mail address: pw96@cornell.edu (P. Wang).

1385-8947/$ – see front matter © 2010 Elsevier B.V. All rights reserved.
doi:10.1016/j.cej.2010.03.052

extent as uniformly distributed on the molecular level, although there are some signs of non-uniform distribution. These films have well-defined areas and thicknesses and are easy to be studied by electrochemical techniques. The films were characterized using WDS, SEM, AFM/EFM, CV, PSC, and EIS.

2. Materials and methods

Pt electrodes were fabricated using standard photolithographic techniques. The advantages were that a large amount of identical electrodes could be obtained in a single batch and the geometries of the electrodes could be accurately controlled. To start the fabrication, a 500 nm insulation layer of silicon dioxide was deposited on a 4-in. silicon wafer (500 μm thick, single side polished, <1 0 0> crystal orientation) by plasma enhanced chemical vapor deposition (PECVD) (GSI single wafer PECVD, GSI Group Sciences). The lift-off technique was used to define the electrode geometry. Layers of 30 nm of Ti and 130 nm of Pt were electron beam evaporated (CHA Mark 50 e-Beam Evaporator) on the substrate to form the electrodes. Wafers were then coated with a 400 nm capping layer of low stress silicon nitride by PECVD. The active areas and bonding pads were defined by selectively etching the silicon nitride layer using reactive ions (Oxford 81 Etcher, Oxford PlasmaLab 80+ RIE System). The geometry of the active area was chosen to be a 250 μm × 750 μm rectangle. Wafers were diced into chips (Kulicke & Soffa 7100 Dicing Saw). For each chip, bonding pads were connected to insulated fine wires by silver conductive epoxy (MG Chemicals) and then insulated from the environment with regular epoxy (Epoxy 907, Miller-Stephenson).

Prior to use, the electrode surface was electrochemically cleaned in 0.1 M H_2SO_4 solution on a CHI600D electrochemical work station. Ag/AgCl in saturated KCl aqueous solution was used as the reference electrode. The Pt electrode was held at −0.55 V for 30 s and at +2.20 V for another 30 s and then scanned over the range of −0.30 to +2.15 V with a sweep rate of 2.00 V/s for 5 min. Then monomer EDOT (Sigma–Aldrich) was electrochemically polymerized and deposited onto the Pt electrode surface. In this process, Nafion anions in the solution were incorporated into the film as doping species to maintain charge neutrality. Specifically, PEDOT/Nafion was synthesized from a Nafion perfluorinated resin solution (Sigma–Aldrich, 5% in mixture of lower aliphatic alcohols and water, contains 45% water, hydrogen ion form) with an EDOT concentration of 0.01 M under galvanostatic mode with a current density of 0.5 mA/cm^2. The electrical current was supplied by a Gamry FAS2 Potentiostat/Galvanostat. Chronopotentiometric curves were recorded during electrochemical polymerization. The polymerization was performed in either three-electrode or two-electrode configuration. In both configurations, the thin-film Pt electrode was used as the working electrode. In the three-electrode configuration, Ag/AgCl was used as the reference electrode and a Pt wire was used as the counter electrode. In the two-electrode configuration, a Pt wire was used simultaneously as the reference electrode and the counter electrode. Each time prior to use, the Pt wires were polished by sandpaper and rinsed with deionized (DI) water.

WDS was performed using a JEOL 8900 Electron Probe Microanalyzer to verify the successful incorporation of Nafion into the films. SEM and AFM/EFM were utilized to characterize the surface structures and compositions of the films. SEM was conducted on a Leica 440 scanning electron microscope. AFM/EFM was conducted on a Veeco Dimension 3100 Ambient AFM system employing a cantilever with conductive coating (Veeco, MESP-LM).

CV was performed to test the electrochemical activity of the film. Deoxygenated phosphate buffered saline (PBS) solution (pH = 7.4) was used as the electrolyte in a three-electrode configuration. The Pt electrodes with PEDOT/Nafion films were used as the working electrodes. Ag/AgCl in saturated KCl aqueous solution was used as the reference electrode. A Pt wire was used as the counter electrode. A scan rate of 0.1 V/s was used and the behavior of the working electrode was studied within a wide potential range between −0.1 and +1.5 V. Yet this limit was narrow enough to remain in the water window. PSC measurements were carried out with the same experimental set-up as in CV measurements.

In the EIS study, deoxygenated PBS solution (pH = 7.4) was used as the electrolyte in a three-electrode configuration. The Pt electrodes with PEDOT/Nafion films were used as the working electrodes. Ag/AgCl was used as the reference electrode, and a coiled Pt wire as the counter electrode. A 5 mV (rms) driving AC sinusoid was used as the input signal with the DC potential set to −0.10, +0.25, or +0.60 V versus Ag/AgCl. The value of the impedance was measured at five discrete frequencies per decade over the range of 0.25 to 10^4 Hz. The electrochemical modeling software Gamry Echem Analyst was used for equivalent circuit modeling.

3. Results and discussion

Prior to electrochemical polymerization, the cleanliness of the Pt surface was tested by cyclic voltammetry in N_2 saturated 0.1 M H_2SO_4 solution over the range of −0.2 to +1.32 V at a sweep rate of 0.1 V/s. Hydrogen adsorption/desorption peaks were used to calculate the microscopic surface area of the Pt electrode. In our calculation, we excluded double-layer capacitive charge and used a conversion factor of 210 μC/cm^2 [12]. The roughness factor was determined to be 1.67, which revealed that the Pt electrode surface was rather smooth and thus had a well-defined geometry.

The electrochemical polymerization method allows for precise control of polymer film growth on electrode sites. The growth rate is directly proportional to the current density and the film thickness can be controlled by duration of electrical current supply. Monomer concentration in the solution could also affect deposition process and film property. The solubility of EDOT in mixture of aliphatic alcohols and water (approximately 1:1) should be fairly high since aliphatic alcohols are good polar organic solvents. The traditional solvent for EDOT polymerization was acetonitrile or mixture of acetonitrile and water. However, solid Nafion is chemically inert and difficult to be dissolved in a solvent. Thus we chose the commercially available Nafion solution to avoid the potential difficulty and complexity. There were concerns that part of the current was consumed to oxidize aliphatic alcohols during the deposition process and the by-products could be incorporated into the film as impurities. However, it is very unlikely that these side reactions happened during our experiments. We chose 0.01 M EDOT concentration, 0.5 mA/cm^2 current density and 3.5 min deposition time as our “model system”. The choice of the current density was based on the parameters used and results reported in Refs. [3,13]. Under potentiostatic polymerization mode, dominant growth of polymer around the perimeter of the electrode was observed. In contrast, galvanostatic mode could give us much better control of the film smoothness and uniformity and thus would lead to well-defined film geometry. The above polymerization conditions lead to an average film thickness of 874 nm measured by profilometry. It has been shown that application of 22 mC/cm^2 corresponded to 100 nm polythiophene film [14]. By using this conversion factor, we were able to calculate the theoretical film thickness to be 477 nm. From this estimation we could infer that side reactions in the polymerization process were suppressed to a minimal extent. Instead of “missing charge”, there was “missing film thickness”. The discrepancy between the measured and theoretical film thickness can be reconciled by recognizing that the correspondence between 22 mC/cm^2 and 100 nm film thickness was for polythio-

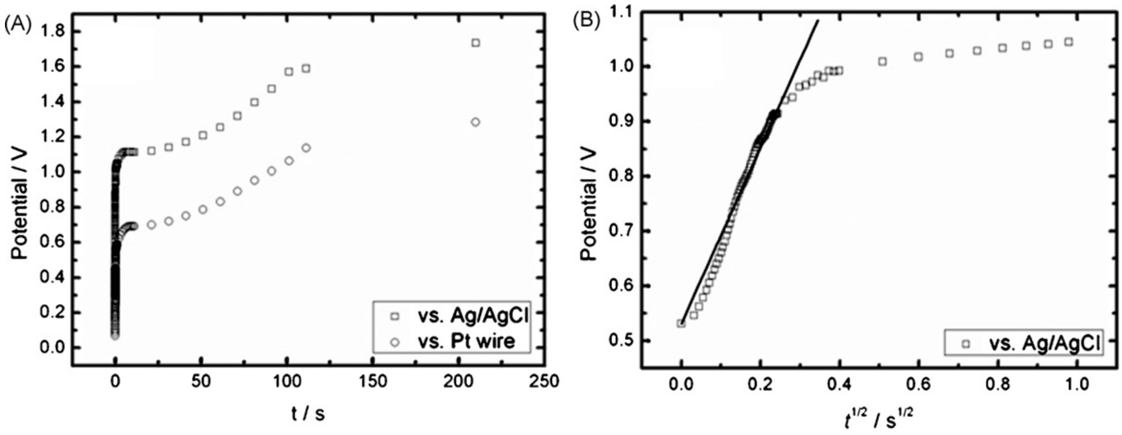

Fig. 1. (A) Chronopotentiometric curves recorded during electrochemical polymerization and (B) plot of potential versus $t^{1/2}$.

phene in general. From our measurement, this conversion factor for PEDOT/Nafion system turned out to be 12 mC/cm^2. Chronopotentiometric curves were also recorded during polymerization. As can be seen in Fig. 1A, the two chronopotentiometric curves differ from each other only by a constant shift in potentials. Since the Pt wire set-up is much simpler than the Ag/AgCl set-up, we chose it for large quantity synthesis. But we will use the potentials versus Ag/AgCl for discussions throughout the paper. After the current was switched on, the potential quickly increased from the open circuit value of ca. +0.53 V to a quasi-steady-state value of +1.1 V (the plateau from 1 to 30 s). For a totally irreversible reaction, the potential at short times should have a linear dependence on $t^{1/2}$ with the intercept being the open circuit potential (Fig. 1B). After the sharp increase regime and the short plateau regime, the potential curve entered the slow increase regime. The current was maintained at constant value and the gradual increase in overpotential came from the gradual concentration depletion of the reactant monomer at the electrode surface [12]. Also notice that there was a kink at around $t = 100$ s, which indicated a discontinuous change in the physical and electrochemical properties of the system such as film structure and morphology, interfacial charge transport mechanism, and polymer growth mode.

In their oxidized states, conducting polymers exist as polycations with delocalized positive charges along their conjugated backbones. During electrochemical polymerization, negatively charged counter ions in the electrolyte are incorporated through electrostatic interactions into the film to maintain charge balance. The existence of Nafion in the film was confirmed by WDS technique. We took advantage of the fact that the chemical element fluorine is present in Nafion but absent in PEDOT. Fig. 2B shows

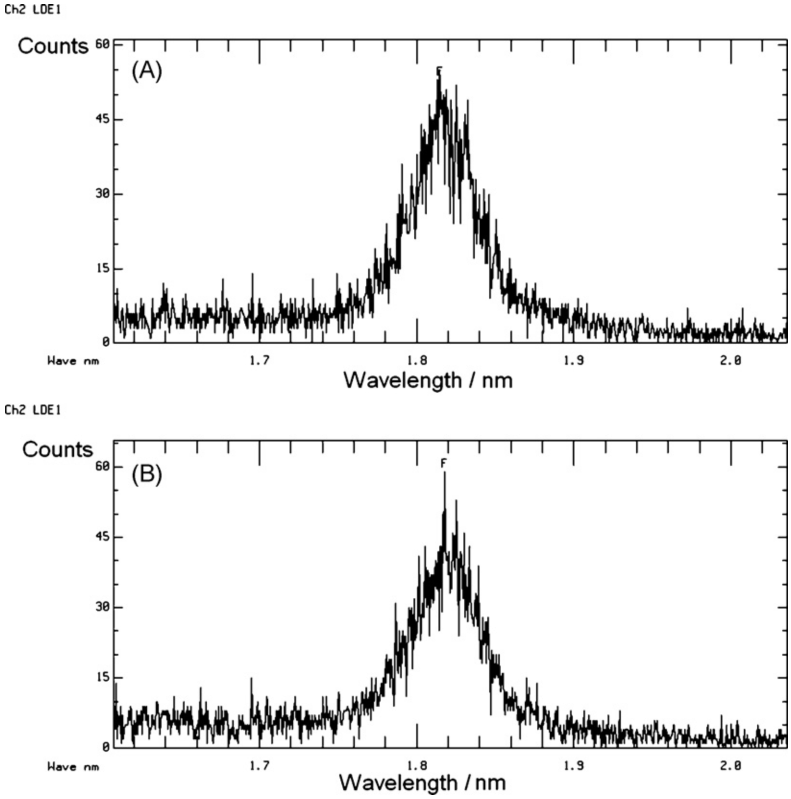

Fig. 2. (A) WDS spectrum of the as-synthesized film and (B) WDS spectrum of synthetic CaF_2. The horizontal axis is detected X-ray wavelength in nm and the vertical axis is counts.

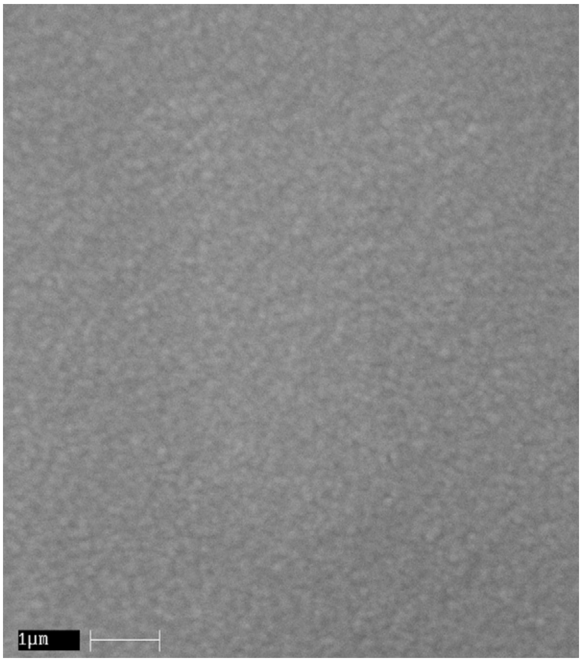

Fig. 3. SEM image of the surface of the PEDOT/Nafion film. The scale bar in the picture represents 1 µm.

the WDS spectrum of the as-synthesized film while Fig. 2A shows that of synthetic CaF_2 (Harshaw Chemical Corp.) used as standard for fluorine. The spectrums have unambiguously confirmed that Nafion has been successfully incorporated into the film.

A detailed view of the PEDOT/Nafion film's morphology by SEM is shown in Fig. 3. For the magnification used in taking this image, the film looks dense and smooth. Deposition of PEDOT with bigger counter ions tends to form denser films. The image also reveals a somewhat fuzzy surface on the scale of 100 nm. Fig. 4 shows the AFM image taken on a 12 µm × 12 µm site area. The needle-like surface structure is obvious in this image. The maximum height of the needle is about 40 nm. Statistical analysis gives R_a of 9.4 nm and R_q of 12.9 nm. Thus the film is rough on the nanometer scale but can be considered smooth on the micron scale.

EFM is used to map the vertical component of the electric field between the tip and the sample versus the in-plane coordinates.

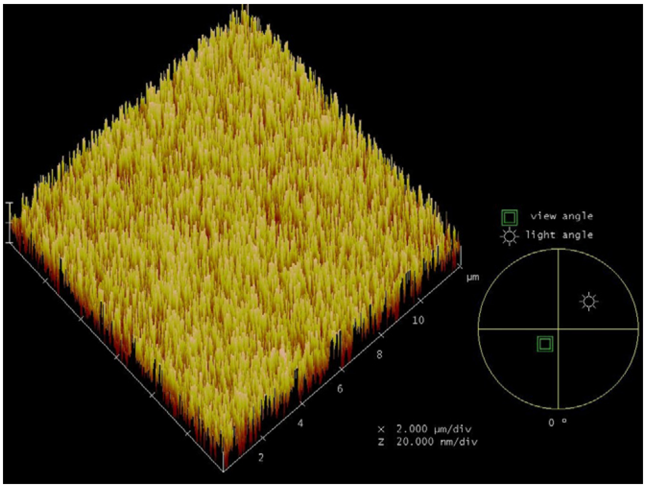

Fig. 4. AFM image of the surface of the PEDOT/Nafion film. The dimension of the image is 12 µm × 12 µm. In the x–y directions one division represents 2 µm and in the z direction one division represents 20 nm.

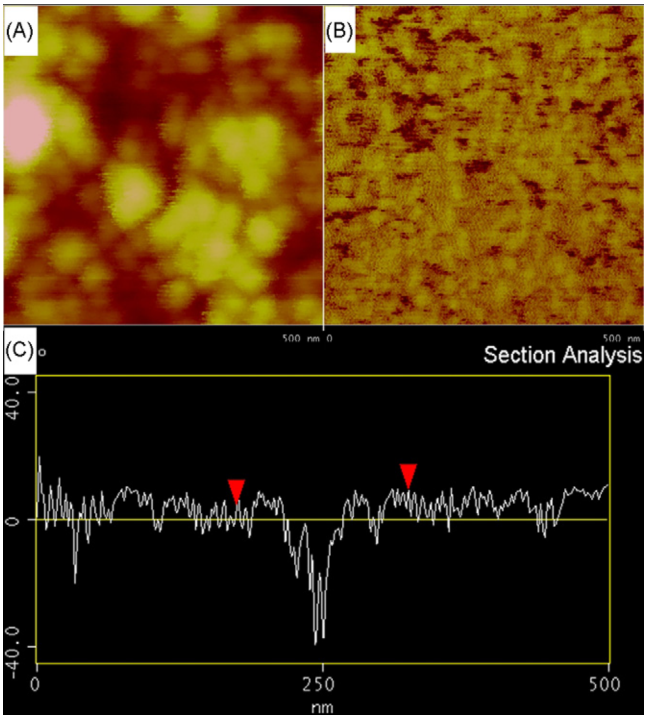

Fig. 5. (A) Topographical image of PEDOT/Nafion film taken on a 500 nm × 500 nm site area; (B) EFM image taken on the same site and (C) sectional analysis of the EFM image.

Since the electric field is also shaped by the surface topography, large differences in topography can make it difficult to distinguish electric field variations. For this reason, two-pass lift-mode measurement has been introduced to separate the electric field variations from the topography contributions. In the first scan, topographical data is taken in tapping mode. The cantilever is then ascended to lift scan height, and a second scan is performed such that the cantilever tip follows stored surface topography at the lift height while responding to electric field influences. In the PEDOT/Nafion film, PEDOT backbones had delocalized mobile holes which were compensated by negative sulfonate groups in Nafion. Therefore, in the PEDOT/Nafion system, the PEDOT-rich region would accumulate positive charges and the Nafion-rich region would accumulate negative charges. When exposed on the surface, these charges would give contrast in an EFM phase image. If the cantilever tip was positively charged (which was used in our experiment), PEDOT-rich region would be reflected as phase advances and Nafion-rich region as phase lags. Fig. 5B shows the EFM image taken on a 500 nm × 500 nm site area. For comparison, Fig. 5A shows the topographical image taken on the same site. In Fig. 5B the yellow regions in the image correspond to charge neutral regions in the film. The bright yellow spots correspond to PEDOT-rich regions with 5–10° phase advances while the dark red spots correspond to Nafion-rich regions with 30–40° phase lags. A typical section analysis of the EFM image is shown in Fig. 5C. It is true that PEDOT and Nafion have not achieved a fully molecular level mixing in the as-synthesized film. We are not sure what might be responsible for this slight phase segregation. One possible explanation is the slight uneven current distribution during electrochemical polymerization due to the surface topography of the underlying Pt electrode. The asymmetry in the magnitudes of phase advances and lags can be interpreted as the consequence of charge delocalization on the PEDOT backbones and charge localization on the Nafion sulfonate groups. Notice that PEDOT is the major component in the composite film and is percolated within the film.

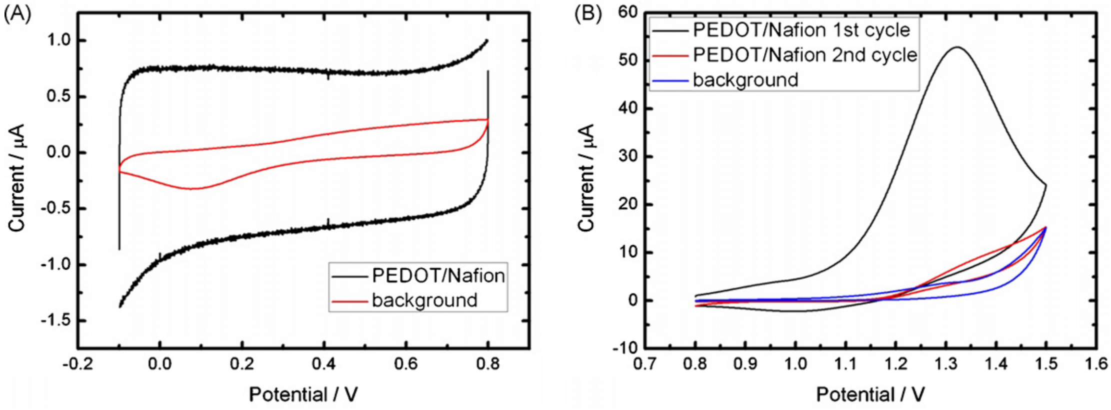

Fig. 6. Voltammograms of PEDOT/Nafion film and bare Pt electrode in the potential range of (A) −0.1 to +0.8 V and (B) +0.8 to +1.5 V.

Electrochemical properties of the PEDOT/Nafion film were examined by CV. Fig. 6A and B shows voltammograms of the PEDOT/Nafion film in the potential range of −0.1 to +0.8 and +0.8 to +1.5 V, respectively, together with the background scans (we use the convention that anodic currents are presented as positive). The background scans were carried out with bare Pt electrodes. The voltammograms of the PEDOT/Nafion film obtained between −0.1 and +0.8 V are broad and structureless. There is no obvious redox peak over this potential range. The rectangular shape of the curve indicates that the film behaves like an electrochemical capacitor. From the encapsulated area by the curves, we can estimate that the electrochemical capacitance of the film is about 8.4 times that of the corresponding bare Pt electrode. The voltammograms of the PEDOT/Nafion film obtained between +0.8 and +1.5 V reveal a salient feature which is a large and virtually irreversible oxidation peak at 1.32 V. Similar peaks have been observed in other PEDOT films [15,16]. Comparison with the background scan indicates that the oxidation peak can be ascribed solely to the polymer. Notice that there is a weak, broad and diffused reduction peak around 1.00 V in the cathodic wave of the first cycle of the PEDOT/Nafion voltammogram. From the second cycle, the voltammogram of the film looks the same to that of the background. The irreversible anodic peak is assigned to PEDOT overoxidation. This process leads to permanent changes in the polymer. The molecular mechanism has been elucidated in detail in Ref. [17]. The polymer chain is broken by overoxidation and the film might peel off, which has been observed in our experiment. It is interesting to notice that water plays an important role in the complete overoxidation of PEDOT [17]. To summarize, the PEDOT/Nafion composite film follows the following oxidation pathway:

$$\mathrm{PEDOT}^{+}\xrightarrow{+e^-}\mathrm{PEDOT}^{0}\xrightarrow{+e^-}\mathrm{degradation}.$$

PSC was utilized for the quantitative analysis on hole transport properties. PSC technique, in which current is recorded with time after the potential is stepped from the open circuit potential to a desired value, has been established as a method in survey of hole transport properties of conducting polymers [18]. The as-synthesized PEDOT/Nafion film had an open circuit potential of around 0.25 V in deoxygenated PBS solution. To eliminate the variation in initial open circuit potential, we electrochemically biased the film at 0.25 V for 1 min prior to PSC measurements. Final stepping potentials of −0.10 and +0.60 V were investigated. In an effort of correcting the double-layer charging effect and singling out the Faradaic current corresponding to PEDOT/Nafion reduction or oxidation induced by hole transportation, we conducted control experiments in which current–time transients were recorded with the bare Pt electrodes while all the other experimental conditions were kept the same as before. This background current was small and had little contribution to the overall current, but we chose to use the background-subtracted signal in our analysis. We proposed a different theoretical model (compared to that in [18]) to interpret the data and extract information on hole mobility (see Appendix A for detailed derivation). Eq. (A9) tells us that at long times $\ln|I|$ should have a linear dependence on t, and D can be calculated from the slope. However, data at long times suffer from small signal to noise ratio. We chose 0.015–0.1 s as the time interval for data fitting. Fig. 7A and B shows the plots of $\ln|I|$ versus t in this time inter-

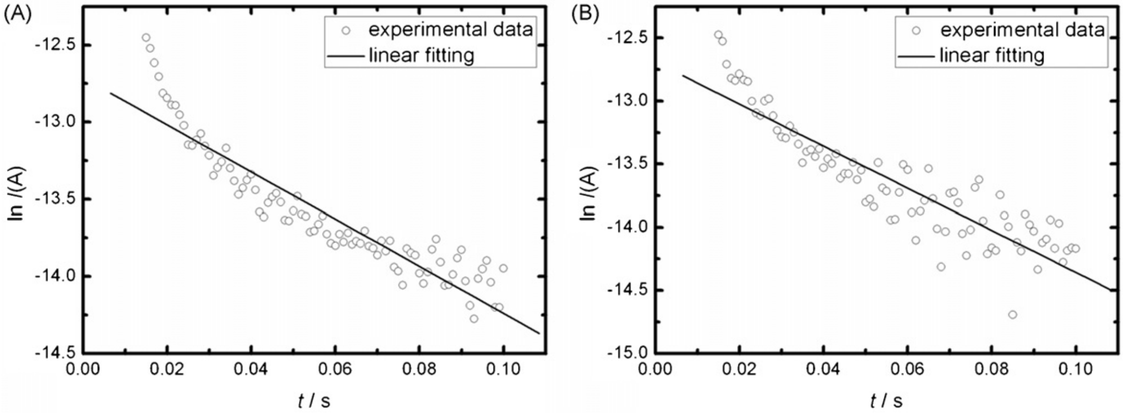

Fig. 7. Plot of $\ln|I|$ versus t from 0.015 to 0.1 s for final stepping potentials of (A) −0.10 V and (B) +0.60 V. The open circles represent measured data and the solid lines represent linear regressions.

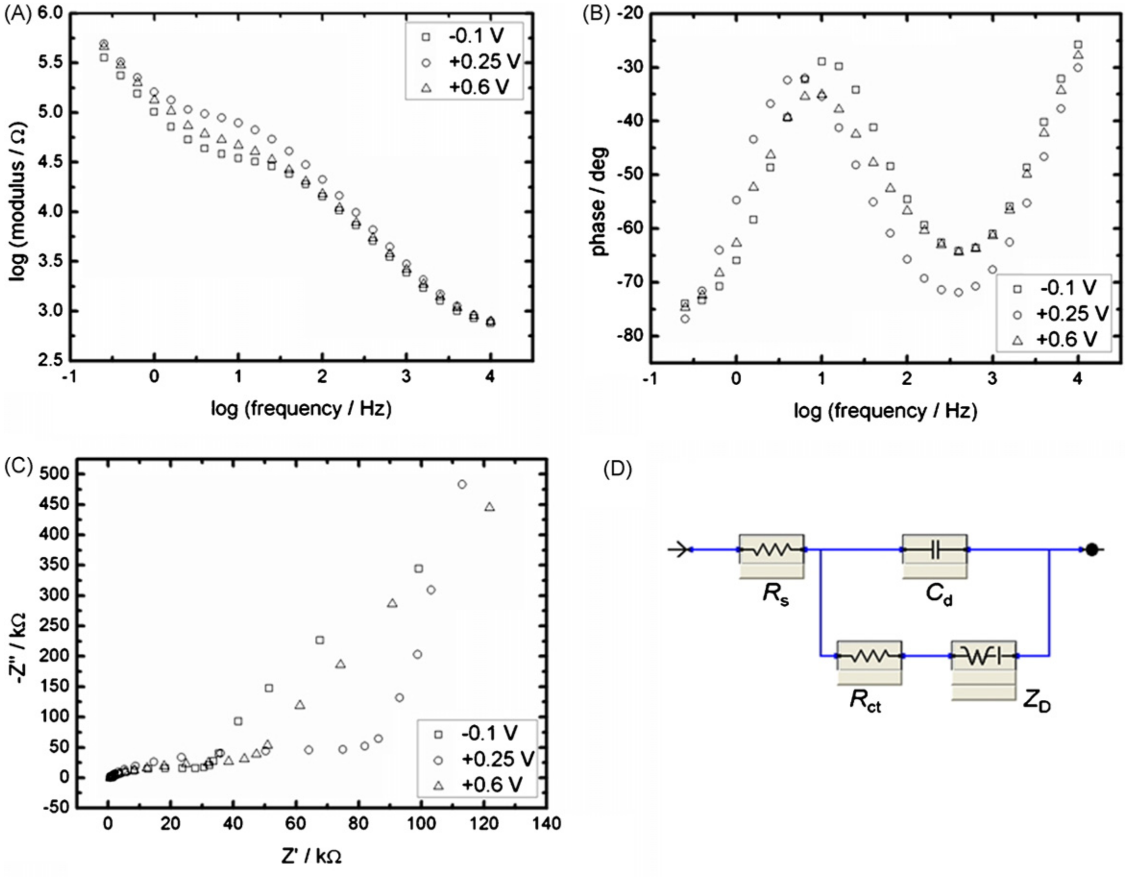

Fig. 8. (A) Bode plot for modulus; (B) Bode plot for phase; (C) Nyquist plot; (D) equivalent circuit.

Table 1
Fitted EIS parameters and calculated diffusion coefficients.

DC potential (V)	R_s (kΩ)	C_d (nF)	R_{ct} (kΩ)	τ_D (s)	C_D (μF)	$D \times 10^{12}$ (m^2/s^{-1})
−0.10	0.739 ± 0.019	69.0 ± 3.3	18.4 ± 0.8	0.119 ± 0.030	1.85 ± 0.15	6.7 ± 1.6
+0.25	0.743 ± 0.021	56.3 ± 1.6	49.4 ± 9.1	0.216 ± 0.023	1.27 ± 0.08	3.6 ± 0.4
+0.60	0.753 ± 0.018	65.0 ± 6.4	12.0 ± 2.2	0.137 ± 0.051	1.40 ± 0.04	6.1 ± 2.1

val for final stepping potentials of −0.10 and +0.60 V, respectively. The open circles represent measured data and the solid lines represent linear regressions. From the slopes of the fitting lines, D was evaluated to be $4.6(\pm 1.3) \times 10^{-12}$ m^2/s and $5.0(\pm 0.8) \times 10^{-12}$ m^2/s, respectively.

Typical impedance spectra obtained for the film are shown in Fig. 8 (Bode plots and Nyquist plots). The general shapes of the impedance plots are distinct from those observed in other PEDOT systems [3,10,11,13,19,20]. In the frequency range studied, the phase plot exhibits a maximum and a minimum. The impedance magnitudes at −0.10, +0.25, and +0.60 V converge at high frequency. In the Nyquist plots, the +0.25 V curve surpasses the −0.10 and +0.60 V curves in the $-Z''$ direction at low frequencies. These features in the EIS data were observed reproducibly. Compared to other PEDOT systems, the PEDOT/Nafion system exhibits richer and more complex EIS behaviors. More systematic studies will be treated in detail in a separate paper. The discussion below is focused on how to extract diffusion coefficients from EIS data. An equivalent circuit approach was used to analyze the EIS data. Often, an equivalent circuit model which fits the EIS data can give some insights into the involved physical and electrochemical mechanisms. Several electrical circuits were initially tested by non-linear least-squares fitting of the experimental data. Classically, the equivalent circuit for a conductive polymer coated metal electrode consists of three elements connected in series: a resistor, a finite-length Warburg diffusion impedance, and a capacitor [3,20]. However, due to the complex EIS behaviors of the PEDOT/Nafion system (especially the S-shape in the impedance phase plots), this classical circuit cannot be used to generate acceptable fitting. The equivalent circuit shown in Fig. 8D was finally chosen to model the system [12]. R_s represents the uncompensated solution resistance, C_d represents the double-layer capacitance, R_{ct} represents the charge transfer resistance, and Z_D represents the finite-length Warburg diffusion impedance. Such an equivalent circuit was found to be able to reproduce the S-shape in the impedance phase plots and give acceptable fittings except near the low frequency end of the spectra. The average error (χ^2-value) of the fittings was 0.010. Notice in the Nyquist plot that in the low frequency range the observed impedance curve deviates from a vertical line. Meanwhile the equivalent circuit predicts an asymptotic pure capacitive behavior in the low frequency range. These problems associated with data fitting in the low frequency range have also been found in other PEDOT systems [20]. The finite-length Warburg diffusion impedance Z_D is characterized by the diffusional time constant τ_D and the diffusional pseudocapacitance C_D, as described by Macdonald [21]:

$$Z_D = (\tau_D/C_D)\cot h(j\omega\tau_D)^{1/2}/(j\omega\tau_D)^{1/2} \tag{1}$$

where j is the imaginary unit $\sqrt{-1}$, ω is the angular frequency and is equal to $2\pi f$. In this work, Z_D is interpreted as the hole transport impedance and is thus related to hole mobility in the film. The diffusional time constant τ_D is related to the diffusion length L and the diffusion coefficient D as follows:

$$\tau_D = \frac{L^2}{D} \tag{2}$$

Assuming that the thickness of the film is the diffusion length L, we can estimate the diffusion coefficient D. Table 1 summarizes the fitted EIS parameters and calculated diffusion coefficients. In all the cases, the uncompensated solution resistances are the same since the same electrolyte and electrochemical cell were used in the experiments. The potential dependence of C_d, R_{ct}, τ_D, C_D, and D is complex and will be investigated further in a separate paper. Notice that the EIS technique was able to measure the diffusion coefficient near the open circuit potential (ca. +0.25 V) where the PSC technique fails. The estimated diffusion coefficients at −0.10 and +0.60 V from EIS measurements are, within experimental errors, consistent with those calculated from PSC measurements.

4. Conclusions

A dense and smooth film of PEDOT/Nafion was prepared on well-fined Pt electrode surface by electrochemical polymerization from an EDOT/Nafion containing solution. Wavelength dispersive X-ray spectrum confirmed the successful incorporation of Nafion into the film. EFM images revealed that PEDOT and Nafion distributed evenly on the nanometer scale while there were slight phase segregations. Cyclic voltammograms revealed a PEDOT/Nafion stable potential window and a PEDOT/Nafion overoxidation potential window. The average diffusion coefficient of hole carriers in the film was evaluated to be $4.8 \times 10^{-12}\,\mathrm{m^2/s}$ by the PSC technique, consistent with the diffusion coefficient estimated from the EIS technique.

Acknowledgement

Peng Wang would like to thank John Hunt for technical help and discussion.

Appendix A.

We treat the process following the potential step as hole diffusion inside the PEDOT/Nafion film. The process can be viewed as charge propagation from the Pt electrode surface which acts as source or sink of holes. Mathematically, the transport can be described in terms of the diffusion equation:

$$\frac{\partial n}{\partial t} = D\nabla^2 n \tag{A1}$$

where n is the number density of holes, and D is the diffusion coefficient of holes.

The thickness of the film is small compared to the lateral dimension of the film and the roughness of the Pt/polymer interface and polymer/solution interface is small compared to the thickness of the film. We establish a Cartesian coordinate system with x-axis perpendicular to the film and y–z plane coincident with the Pt/polymer interface. Furthermore, we denote the film thickness as L. The governing equation and initial and boundary conditions can be written as

$$\frac{\partial n}{\partial t} = D\frac{\partial^2 n}{\partial x^2} \tag{A2}$$

$$\text{At } t = 0, \quad n = n_{initial} \tag{A3}$$

$$\text{At } x = 0, \quad n = n_{final} \tag{A4}$$

$$\text{At } x = L, \quad \frac{\partial n}{\partial x} = 0 \tag{A5}$$

where $n_{initial}$ and n_{final} are the initial and final (infinite time) number densities of holes. Boundary condition (A5) reflects the fact that holes cannot diffuse into the solution.

The dynamic behavior and spatial profile of the number density are presented in Eq. (A6):

$$n = n_{final} + \sum_{n=0}^{\infty} \frac{(n_{initial} - n_{final})\sqrt{2L}}{(n+(1/2))\pi} e^{-D\lambda_n^2 t}\Phi_n(x) \tag{A6}$$

where $\lambda_n = (n+(1/2))\pi/L$, and $\Phi_n(x) = \sqrt{2/L}\sin[(n+(1/2))(\pi x/L)]$.

The electrical current can be computed by

$$I = -\frac{AFD}{N_{\mathrm{A}}} \left.\frac{\partial n}{\partial x}\right|_{x=0} \tag{A7}$$

where A is the area of the electrode, F is Faraday's constant and N_{A} is Avogadro's number.

After some algebra, we have

$$I = \frac{2AFD(n_{final} - n_{initial})}{N_{\mathrm{A}}L} \sum_{n=0}^{\infty} e^{-D\lambda_n^2 t} \tag{A8}$$

At long times

$$I \simeq \frac{2AFD(n_{final} - n_{initial})}{N_{\mathrm{A}}L} e^{-D\lambda_0^2 t} \tag{A9}$$

n_{final} can be either greater or smaller than $n_{initial}$, thus I can be either a positive anodic current or a negative cathodic current.

Eq. (A9) tells us that at long times $\ln|I|$ should have a linear dependence on t and D can be calculated from the slope.

References

[1] G. Heywang, F. Jonas, Poly(alkylenedioxythiophene)s-new, very stable conducting polymers, Adv. Mater. 4 (1992) 116–118.

[2] W. Feng, Y. Li, J. Wu, H. Noda, A. Fujii, M. Ozaki, K. Yoshino, Improved electrical and optical properties of poly(3,4-ethylenedioxythiophene) via ordered microstructure, J. Phys.: Condens. Matter 19 (2007) 186220–186228.

[3] X. Cui, D.C. Martin, Electrochemical deposition and characterization of poly(3,4-ethylenedioxythiophene) on neural microelectrode arrays, Sens. Actuators B 89 (2003) 92–102.

[4] B.L. Groenendaal, F. Jonas, D. Freitag, H. Pielartzik, J.R. Reynolds, Poly(3,4-ethylenedioxythiophene) and its derivatives: past, present, and future, Adv. Mater. 12 (2000) 481–494.

[5] A.M. Nardes, On the conductivity of PEDOT:PSS thin films, Doctoral Dissertation in the Department of Applied Physics, Eindhoven University of Technology, Eindhoven, Netherlands, 2007.

[6] M.C. Morvant, J.R. Reynolds, In situ conductivity studies of poly(3,4-ethylenedioxythiophene), Synth. Met. 92 (1998) 57–61.

[7] M. Dietrich, J. Heinze, G. Heywang, F. Jonas, Electrochemical studies on poly(3,4-ethylenedioxythiophene) and related materials, J. Electroanal. Chem. 368 (1994) 87–90.

[8] H. Yamato, M. Ohwa, W. Wernet, Stability of polypyrrole and poly-(3,4-ethylenedioxythiophene) for biosensor application, J. Electroanal. Chem. 397 (1995) 163–170.

[9] T.D. Gierke, W.S. Hsu, The cluster-network model of ion clustering in perfluorosulfonated membranes, in: A. Eisenberg, H.L. Yeager (Eds.), Perfluorinated Lonomer Membranes, ACS Symp. Ser., vol. 180, American Chemical Society, Washington, DC, 1982, pp. 283–307.

[10] S.J. Higgins, K.V. Lovell, R.M.G. Rajapakse, N.M. Walsby, Grafting and electrochemical characterisation of poly-(3,4-ethylenedioxythiophene) films, on Nafion and on radiation-grafted polystyrenesulfonate-polyvinylidene fluoride composite surfaces, J. Mater. Chem. 13 (2003) 2485–2489.

[11] L. Li, J.F. Drillet, R. Dittmeyer, K. Juttner, Formation and characterization of PEDOT-modified Nafion 117 membranes, J. Solid State Electrochem. 10 (2006) 708–713.

[12] A.J. Bard, L.R. Faulkner, Electrochemical Methods, John Wiley & Sons, Inc., New Jersey, 2001.

[13] Y. Xiao, X. Cui, J.M. Hancock, M. Bouguettaya, J.R. Reynolds, D.C. Martin, Electrochemical polymerization of poly(hydroxyethylated-3,4-ethylenedioxythiophene) (PEDOT-MeOH) on multichannel neural probes, Sens. Actuators B 99 (2004) 437–443.

[14] R.J. Waltman, J. Bargon, A.F. Diaz, Electrochemical studies of some conducting polythiophene films, J. Phys. Chem. 87 (1983) 1459–1463.
[15] G. Zotti, S. Zecchin, G. Schiavon, Conductive and magnetic properties of 3,4-dimethoxy- and 3,4-ethylenedioxy-capped polypyrrole and polythiophene, Chem. Mater. 12 (2000) 2996–3005.
[16] A. Zykwinska, W. Domagala, B. Pilawa, M. Lapkowski, Electrochemical overoxidation of poly(3,4-ethylenedioxythiophene)-PEDOT studied by means of in situ ESR spectroelectrochemistry, Electrochim. Acta 50 (2005) 1625–1633.
[17] U. Barsch, F. Beck, Anodic overoxidation of polythiophenes in wet acetonitrile electrolytes, Electrochim. Acta 41 (1996) 1761–1771.
[18] D. Wakizaka, T. Fushimi, H. Ohkita, S. Ito, Hole transport in conducting ultrathin films of PEDOT/PSS prepared by layer-by-layer deposition technique, Polymer 45 (2004) 8561–8565.
[19] Y.H. Xiao, X.Y. Cui, D.C. Martin, Electrochemical polymerization and properties of PEDOT/S-EDOT on neural microelectrode arrays, J. Electroanal. Chem. 573 (2004) 43–48.
[20] J. Bobacka, A. Lewenstam, A. Ivaska, Electrochemical impedance spectroscopy of oxidized poly(3,4-ethylenedioxythiophene) film electrodes in aqueous solutions, J. Electroanal. Chem. 489 (2000) 17–27.
[21] J.R. Macdonald, Impedance Spectroscopy, Wiley, New York, 1987.